Cell, Vol. 121, 873–885, June 17, 2005, Copyright ©2005 by Elsevier Inc. DOI 10.1016/j.cell.2005.04.031

Physical Association and Coordinate Function of the H3 K4 Methyltransferase MLL1 and the H4 K16 Acetyltransferase MOF

Yali Dou,[1] Thomas A. Milne,[2,4] Alan J. Tackett,[3] Edwin R. Smith,[2] Aya Fukuda,[1] Joanna Wysocka,[2] C. David Allis,[2] Brian T. Chait,[3] Jay L. Hess,[4] and Robert G. Roeder[1,*]

[1]Laboratory of Biochemistry and Molecular Biology
[2]Laboratory of Chromatin Biology
[3]Laboratory of Mass Spectrometry and Gaseous Ion Chemistry
The Rockefeller University
New York, New York 10021
[4]Department of Pathology and Laboratory Medicine
University of Pennsylvania School of Medicine
Philadelphia, Pennsylvania 19104

Summary

A stable complex containing MLL1 and MOF has been immunoaffinity purified from a human cell line that stably expresses an epitope-tagged WDR5 subunit. Stable interactions between MLL1 and MOF were confirmed by reciprocal immunoprecipitation, cosedimentation, and cotransfection analyses, and interaction sites were mapped to MLL1 C-terminal and MOF zinc finger domains. The purified complex has a robust MLL1-mediated histone methyltransferase activity that can effect mono-, di-, and trimethylation of H3 K4 and a MOF-mediated histone acetyltransferase activity that is specific for H4 K16. Importantly, both activities are required for optimal transcription activation on a chromatin template in vitro and on an endogenous MLL1 target gene, *Hox a9*, in vivo. These results indicate an activator-based mechanism for joint MLL1 and MOF recruitment and targeted methylation and acetylation and provide a molecular explanation for the closely correlated distribution of H3 K4 methylation and H4 K16 acetylation on active genes.

Introduction

Many of the changes in chromatin structure induced by transcription factors involve complex patterns of histone modifications by enzymes such as histone acetyltransferases (HATs), histone methyltransferases (HMTs), and kinases. Plasticity in transcription regulation and coupled biological processes can be achieved by dynamic regulation of these histone modifications. The varying format of chromatin modifications has led to the hypothesis of a histone code, which suggests that specific combinations of histone modifications dictate specific transcriptional responses and cellular functions (Strahl and Allis, 2000; Turner, 2002). Thus, it is well established that transcriptionally active, euchromatic regions of the eukaryotic genomes are marked by hyperacetylation of all four core histones, while gene-poor, transcriptionally inactive heterochromatin regions exhibit hypoacetylation (Vaquero et al., 2003). The mechanistic basis for this was revealed by the discovery that many transcriptional coactivators, such as GCN5, p300/CBP, and MOF, proved to be histone acetyltransferases (Carrozza et al., 2003). The effects of histone acetylation are probably additive, given the lack of site specificity for most HATs, with the H4 K16 acetylation catalyzed by MOF and its homologs being among the exceptions (Carrozza et al., 2003; Dion et al., 2005). Recent studies show that acetylation of H4 K16 is critical for chromatin decondensation (Corona et al., 2002) and gene activation in the X chromosome of male *Drosophila* (Smith et al., 2001). There also is accumulating evidence that H4 K16 acetylation may be the founding acetylation event on histone H4 (Smith et al., 2003; Turner et al., 1992; Zhang et al., 2002).

Another histone modification strongly correlated with transcription activation in a wide variety of eukaryotic systems is H3 K4 methylation, especially the trimethylated state (Santos-Rosa et al., 2002; Strahl et al., 1999). Histone acetylation and H3 K4 methylation not only are functionally correlated but also physically linked, as demonstrated by the preferential localization of trimethylated K4 residues in hyperacetylated H3 (Zhang et al., 2004). This strongly suggests that the enzymatic machineries that add these two marks may function in a synergistic manner and, potentially, interact with each other. This notion is supported by demonstrations of physical interactions between Trithorax (TRX) and CBP in *Drosophila* (Petruk et al., 2001) and a transient interaction between MLL1 and CBP in human cells (Ernst et al., 2001). The mechanism underlying the synergism between histone acetylation and H3 K4 methylation, and its functional implications, remain to be elucidated.

Studies to date have described a number of mammalian H3 K4 methyltransferases (Sims et al., 2003). MLL1, of interest here, is the product of a protooncogene that was first detected through chromosomal translocations directly associated with aggressive lymphoid and myeloid acute leukemias, especially among infants (Hess, 2004). MLL1 has been implicated in Hox gene regulation in early embryogenesis (Yu et al., 1995) and, more recently, in the regulation of non-Hox genes such as *p27 (Kip1)* and *p18 (Ink4C)* (Milne et al., 2005). Consistent with its proposed role in transcriptional regulation through modification of histones, chromatin immunoprecipitation (ChIP) assays have shown accumulation of MLL1 and corresponding H3 K4 methylation marks on active target genes (Milne et al., 2002).

Among the known H3 K4 methyltransferases in mammals, several (hSET1 MLL1, MLL2) have been found in large complexes (Goo et al., 2003; Hughes et al., 2004; Nakamura et al., 2002; Wysocka et al., 2003; Yokoyama et al., 2004). While sharing some subunits (e.g., Ash2L and WDR5), these complexes nevertheless contain unique sets of proteins that suggest nonoverlapping functions. In the case of MLL1, one study reported that proteins from six different complexes associated with MLL1 to form a single stable "supercomplex" (Nakamura et al., 2002). This complex was shown to have

*Correspondence: roeder@mail.rockefeller.edu

a K4 methyltransferase activity, but which was much weaker than that of the recombinant MLL1 SET domain and unable to use dimethyl H3 K4 as substrate. A subsequent study reported a much smaller MLL1-HCF complex (six components in addition to MLL) with only minimal overlap with the supercomplex but failed to show any enzymatic activity of the complex (Yokoyama et al., 2004).

To understand the function and mechanism of MLL1 H3 K4 methyltransferase activity in transcriptional regulation, we set out to purify an MLL1-containing complex for functional analysis in our chromatin-based in vitro transcription assays (An et al., 2002). Given the presence in the MLL1 supercomplex of an ortholog (WDR5) to a component in the yeast SET1 complex (Krogan et al., 2002), we developed an immunoaffinity purification procedure based on expression in HeLa cells of an epitope-tagged WDR5. Surprisingly, our studies have resulted in isolation of a complex that contains not only MLL1, WDR5, and other expected components, but newly isolated components that include, most notably, MOF, the MYST family HAT that specifically acetylates H4 K16. This has led us to investigate and to document a functional connection between the MLL HMT and the MOF HAT activities both in vitro and in vivo.

Results

Purification and Characterization of an MLL1-WDR5 Complex

After establishment of a HeLa cell line that stably expresses Flag-tagged WDR5 (f-WDR5), derived nuclear extracts were subjected to a three step purification (with MLL1 monitored by immunoblot) that involved conventional column chromatography on phosphocellulose (P11) and SP Sepharose, followed by immunoaffinity purification on anti-Flag antibody (M2 agarose) beads (Figure 1A). Although WDR5 is common to MLL1 (Nakamura et al., 2002; Yokoyama et al., 2004), MLL2 (Hughes et al., 2004), and hSET1/HCF (Wysocka et al., 2003) complexes, the first two steps efficiently separate MLL1 from hSET1 (mostly in the P11 BC300 and SP BC300 fractions) and MLL2 (mostly in P11 BC300 and SP BC300 fractions) and remove most of the unincorporated f-WDR5 protein.

Mass spectrometric analysis of the purified f-WDR5-containing MLL1 complex (designated MLL1-WDR5) revealed 29 proteins (listed alongside the zinc stained polyacrylamide gel, Figure 1B), including the tagged WDR5, that were not present in the parallel mock-purified preparation derived from a conventional HeLa nuclear extract (data not shown). Five of these proteins are uncharacterized proteins in the database. Of the remaining 24 proteins, six were recently reported in the MLL1-HCF complex (Yokoyama et al., 2004). They are the proteolytically derived MLL^N and MLL^C components of MLL1, ASH2L, RbBP5, WDR5, and HCF1. They appear to represent the most tightly associated ("core") components of the MLL1 complex. With the notable exceptions of RbBP5, WDR5, and some TAFs, most of the proteins that were reported in the earlier MLL1 complex preparation (Nakamura et al., 2002) were not detected in our preparation by mass spectrometry or immunoblot (data not shown). The most notable new proteins in our MLL1-WDR5 preparation include TAF components of TFIID, components of the E2F6 subcomplex, and MOF, a MYST family HAT. hSET1 and MLL2 were not detected by mass spectrometry. CBP, which is known to transiently interact with MLL1 (Ernst et al., 2001), also was not detected.

The mass spectrometry results were confirmed by immunoblot using available antibodies. In all cases tested, proteins that were identified by mass spectrometry were confirmed (Figure 2A). Menin, which was found in both the MLL1-HCF complex and the MLL2 complex, was detected by immunoblot even though it was not detected by mass spectrometry. The human ortholog (hMSL1) of *Drosophila* MSL1, which is known to interact with *Drosophila* MOF in the evolutionarily conserved dosage compensation complex (Smith et al., 2000), was not present in the MLL1-WDR5 complex (Figure 2B). Human TIP60, another MYST family HAT that shares sequence similarity with hMOF, also was not detected. Extremely low levels of hSET1 and MLL2 were detected by immunoblot, but, consistent with the separation of most SET1 and MLL2 from MLL1 in the ion exchange steps (above), we were unable to detect any unique components (e.g., Sin3A) of the hSET1 complex (Figure 2B).

Since the finding of hMOF in the MLL1-WDR5 complex has important functional implications, our subsequent studies (described herein) were focused on interactions of MOF with the MLL1-WDR5 complex. Functional characterization of other identified proteins is ongoing (see also below). In further confirmation of the stable association of MOF with the MLL1-WDR5 complex, MOF was found to cosediment on a sucrose gradient with other components (MLL^C, Ash2L, RbBP5, and Ring2) of the three step purified MLL1-WDR5 complex (Figure 2C). The apparent size of the MOF-containing MLL1-WDR5 complex is around 1.5 MDa. Reciprocal immunoprecipitation of the three step purified MLL1-WDR5 complex with anti-MOF antibody also revealed coimmunoprecipitation of MLL1 with other tested components (f-WDR5, RbBP5, and Ring2) of the MLL1-WDR5 complex (Figure 2D). Importantly, TAFs, hSET1, and MLL2 were not detected in the anti-MOF immunoprecipitate. This suggests, for the M2 agarose preparation, that the interactions between MLL1-WDR5 and MOF are specific, that trace levels of hSET1 and MLL2 may reflect contaminating f-WDR5-containing complexes, and that TAFs (presumably as TFIID) are associated with a distinct (MOF-deficient) subfraction of WDR5-containing complex(es). The copurification of MOF with Flag-tagged RbBP5, another component of the MLL1-WDR5 complex, provides further support for a stable association of MOF with the MLL1-WDR5 complex (Figure 2E).

MLL1 and MOF Interact Both In Vivo and In Vitro

To further substantiate intracellular MOF interactions with the MLL1-WDR5 complex, 293T cells were transfected with vectors expressing HA-tagged MLL1 (HA-MLL1) and histidine-tagged MOF (His-MOF). Analysis of derived cell lysates by Ni-NTA chromatography and immunoblot revealed retention of MLL1-HA along with

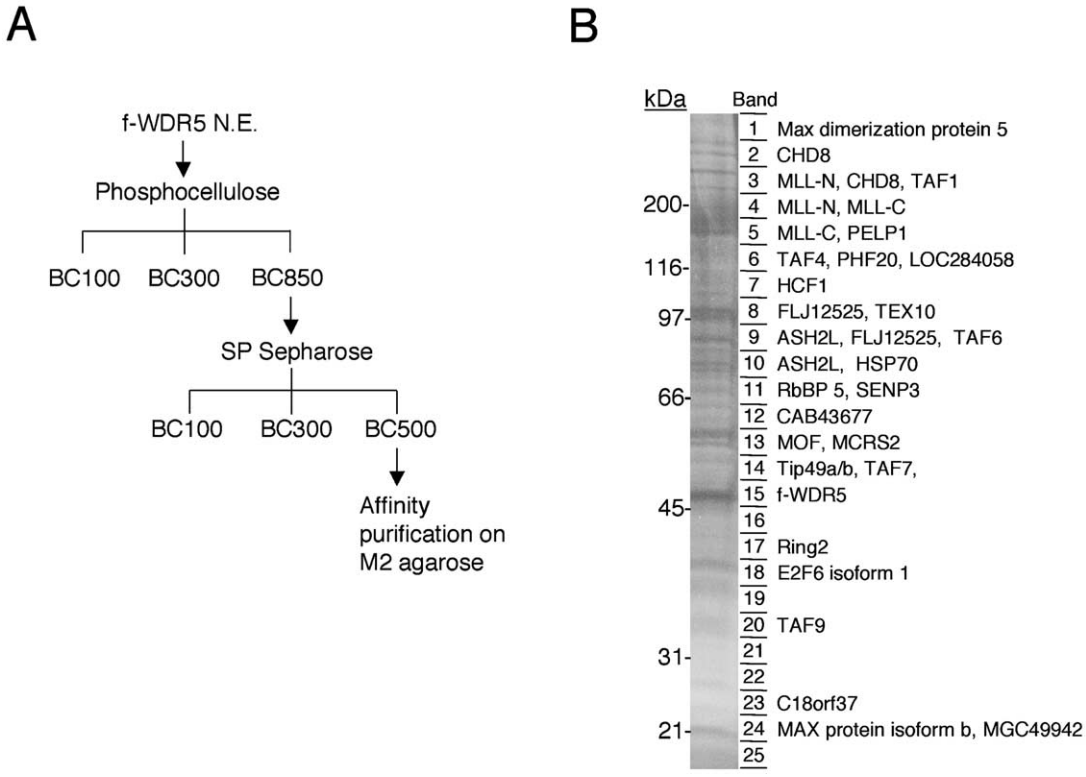

Figure 1. Purification and Mass Spectrometric Analysis of the MLL1-WDR5 Complex

(A) Scheme for three step purification of the MLL1-WDR5 complex.

(B) Zinc-stained 4%–20% gradient gel of proteins eluted from M2 agarose beads. Proteins identified by MALDI mass spectrometry are indicated. Several proteins were recovered from more than one slice.

His-MOF when both were coexpressed but not when either was expressed alone (Figure 3A and data not shown). Similar experiments with HA-MLL1 and His-Ring2, another newly identified member of the MLL1-WDR5 complex, and with HA-MOF and His-Ring2 revealed MLL1-HA binding (Figure 3B) and MOF-HA binding (Figure 3C) in conjunction with His-Ring2. Altogether, these results provide further support for intracellular interactions between MLL1, MOF, and Ring2 and their presence within a common complex.

Incubation of nuclear extract with GST-fused WDR5, RbBP5, and MOF proteins also led to binding of endogenous MLL1 (data not shown), suggesting that MLL1 might serve as a scaffold for direct interaction of these proteins and prompting an analysis of MLL1 domains involved in the interactions. To this end, six MLL1 fragments that cover both the MLL^N region (M1–M4) and the MLL^C region (M5, M6) were generated by in vitro transcription/translation and used in binding assays (Figure 4C). MOF showed the strongest interaction with the M5 fragment that contains the CID domain and a weaker interaction with the M6 fragment that contains the SET domain (Figure 4C). WDR5 and RbBP5 showed similar strong and weak interactions with the M5 and M6 fragments, respectively, but also showed significant interactions with the M2 fragment that contains the DNA methyltransferase homologous region (DNMT). A further analysis with MLL1 M5 subfragments indicated that a region (residues 3100–3300) C-terminal to the CID domain is required for mediating the interaction with MOF (Figure 4D). These results extend a previous study, involving different assays, which suggested that WDR5 and RbBP5 interactions with MLL1 are dependent on (but not necessarily restricted to) the SET domain (Yokoyama et al., 2004).

A similar scheme for mapping MLL1 interacting domains in MOF employed GST fusion proteins containing full length MOF, MOF (1–235) (with deletion of HAT domain), MOF (1–171) (with deletion of both the HAT domain and the zinc finger). Both full-length MOF and MOF (1–235), but not MOF (1–171) lacking the zinc finger, bound the M5 fragment, suggesting that the zinc finger domain is required for the MLL1 interaction (Figure 4E). Similar results were obtained using purified recombinant MLL^C protein for the binding assay, indicating that MOF directly interacts with MLL^C in the MLL1-WDR5 complex (Figure 4E).

The Purified MLL1-WDR5 Complex Has Both HMT and HAT Activities

HMT and HAT activities of the three step purified MLL1-WDR5 complex were assayed using both free histone octamer and either native HeLa or recombinant nucleosomes as substrates. The purified MLL1-WDR5 complex showed robust H3-specific HMT activities on all of these substrates (Figure 5A). When assayed with a free

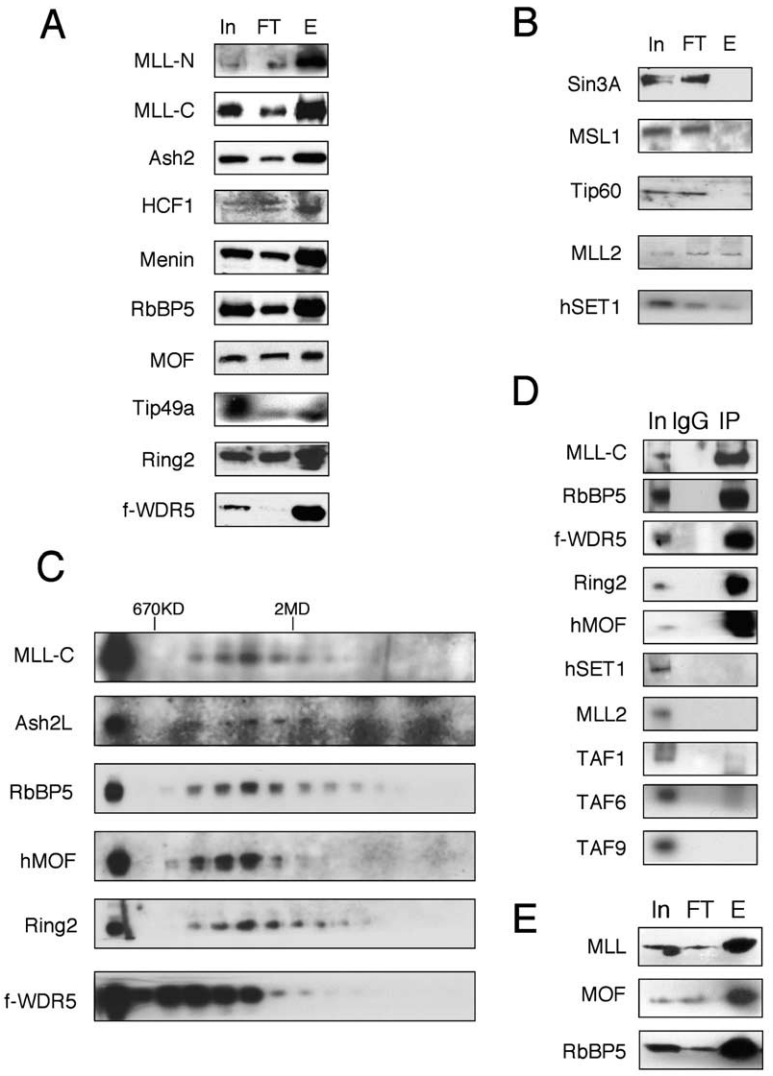

Figure 2. Immunoblot Confirmation of Components of the Purified MLL1-WDR5 Complex

(A) Immunoblot of selected proteins identified by mass spectrometry. In, input, SP Sepharose BC500 fraction; FT, flowthrough; E, elution. Antibodies used in this and other (B–E) blots are indicated on the left.

(B) Immunoblot analysis of select components previously identified in other complexes as controls.

(C) Immunoblot analysis of 3-step purified complex following fractionation by sucrose gradient sedimentation. Sedimentation positions of molecular weight markers are indicated at the top.

(D) Immunoprecipitation (IP) of the three step purified complex by anti-MOF antibodies. Mouse IgG was used for control IP.

(E) Immunoblot analysis of three step purified complex through Flag-RbBP5.

recombinant histone octamer carrying the H3 K4Q mutation, there was no detectable H3 methylation but, instead, a low level of H2B methylation. In contrast, with the more physiological (recombinant) nucleosome substrate carrying the H3 K4Q mutation, all histone methylation was lost (Figure 5A). Hence, the HMT activity is specific for H3 lysine 4 (K4).

To test the substrate specificity of the MLL1-WDR5 complex, H3 peptides that were either non-, mono-, di-, or trimethylated on K4 were used in HMT assays (Figure 5B). All except the trimethylated H3 K4 peptide served as substrates, although the dimethylated H3 K4 peptide was a better substrate than unmodified and monomethylated K4 (Figure 5B). This result differs from that reported with the recombinant SET domain of MLL1, which failed to methylate dimethylated K4 peptides (Milne et al., 2002; Nakamura et al., 2002). The failure of the trimethylated H3 K4 peptide to be further methylated, even though it has unmethylated K9, further demonstrates the K4 specificity of the MLL1-WDR5 complex.

Consistent with the presence of MOF, the purified MLL1-WDR5 complex also has a strong HAT activity. With the free histone octamer substrate, the complex shows a clear substrate preference for histone H4 but also acetylates H3 and H2A (Figure 5C). In contrast, the MLL1-WDR5 complex only acetylates H4 in nucleosomal substrates, thus showing a much greater specificity with the more physiological substrate. The same change in acetylation pattern with different substrates was previously observed for MOF in *Drosophila* (Akhtar and Becker, 2000; Smith et al., 2000). Since MOF in *Drosophila* was shown to specifically acetylate H4 lysine 16 (Akhtar and Becker, 2000; Smith et al., 2000), we also assayed the utilization of this site by the MLL1-WDR5 complex. Using recombinant nucleosomes reconstituted with H4 containing a K16 mutation, acetylation of H4 was dramatically decreased when compared to H4 acetylation on a wild-type H4 nucleosome (Figure 5C).

HMT and HAT Activities of the MLL1-WDR5 Complex Act Coordinately in Transcriptional Regulation

Both H3 K4 trimethylation and H4 K16 acetylation are marks for active transcription (see Introduction). To test the function of the HMT and HAT activities of the MLL1-

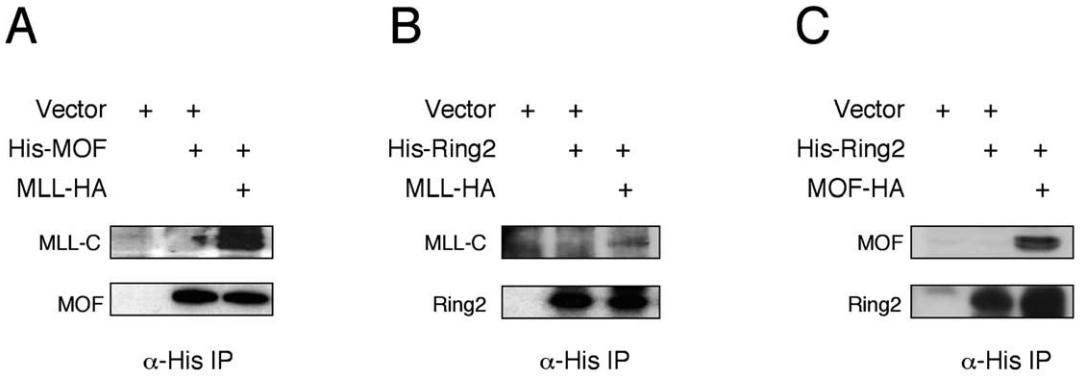

Figure 3. Stable Intracellular Interactions of MLL1 and MOF

293T cells were transiently transfected with expression vectors encoding His-MOF and MLL1-HA (A), His-Ring2 and MLL1-HA (B), or His-Ring2 and MOF-HA (C). For each analysis, proteins eluted from Ni-NTA were monitored by immunoblot with either anti-His or anti-HA antibody.

WDR5 complex in transcription regulation, we turned to our established in vitro transcription system using a recombinant chromatin template assembled with the Acf-1/ISWI/NAP1 system (Figure 6B; An et al., 2004). In this system, activator-mediated transcription is strongly dependent upon recruitment of cofactors that effect histone modifications (An et al., 2004). Our previous demonstration of p53-induced accumulation of H3 K4 methylation on an endogenous p53 target gene (An et al., 2004) raised the possibility that this might be due to MLL1 recruitment by p53. Consistent with this possibility, GST-p53, but not GST alone, was found to effi-

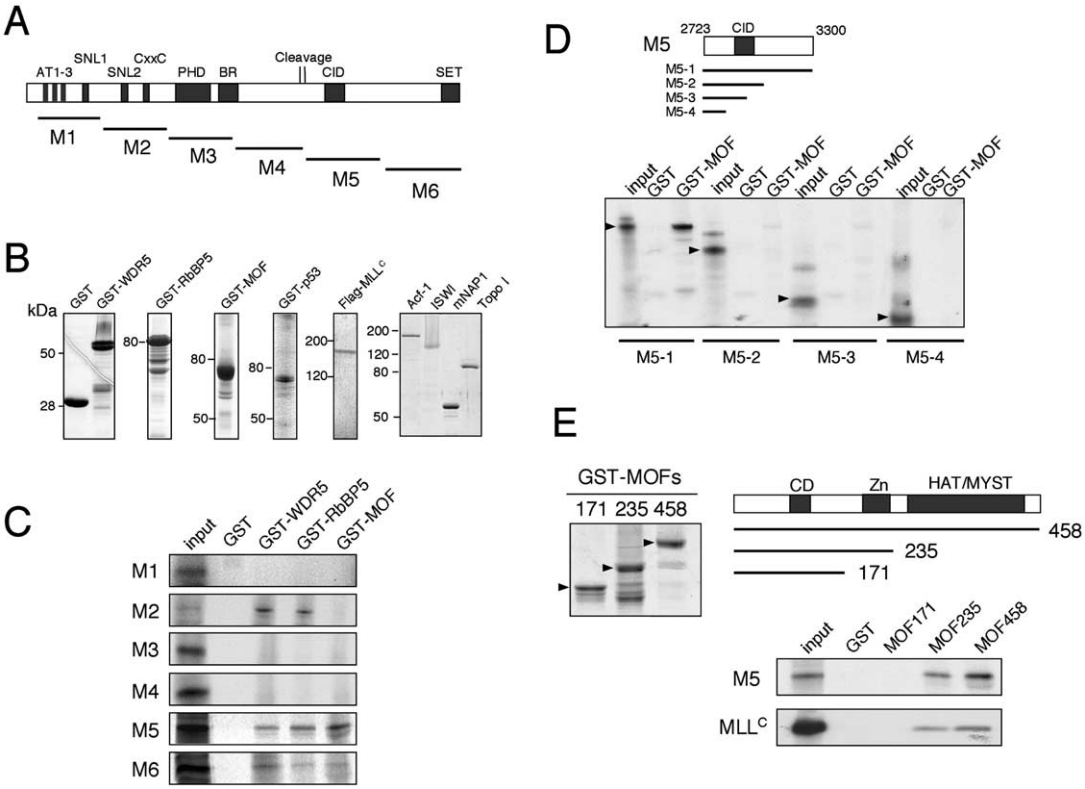

Figure 4. Mapping of MLL1 and MOF Interaction Domains

(A) Schematic representation of MLL1 and derived fragments (see Supplemental Data).

(B) SDS-PAGE analysis of purified recombinant proteins used either for in vitro binding experiments or in the chromatin assembly reaction (see Figure 6B).

(C) Interaction of in vitro-translated, ^{35}S-methionine-labeled MLL1 fragments (indicated on the left) with GST-fusion proteins (indicated at the top).

(D) Interactions of in vitro-translated, ^{35}S-methionine-labeled M5-derived fragments with GST-MOF. Full-size translated proteins in the inputs are indicated by arrowheads.

(E) Interactions of MOF deletion mutants with MLL1 fragments. Indicated GST-MOF fusion proteins were incubated either with an in vitro translated, ^{35}S-methionine-labeled M5 fragment or with a purified recombinant Flag-MLL^C protein.

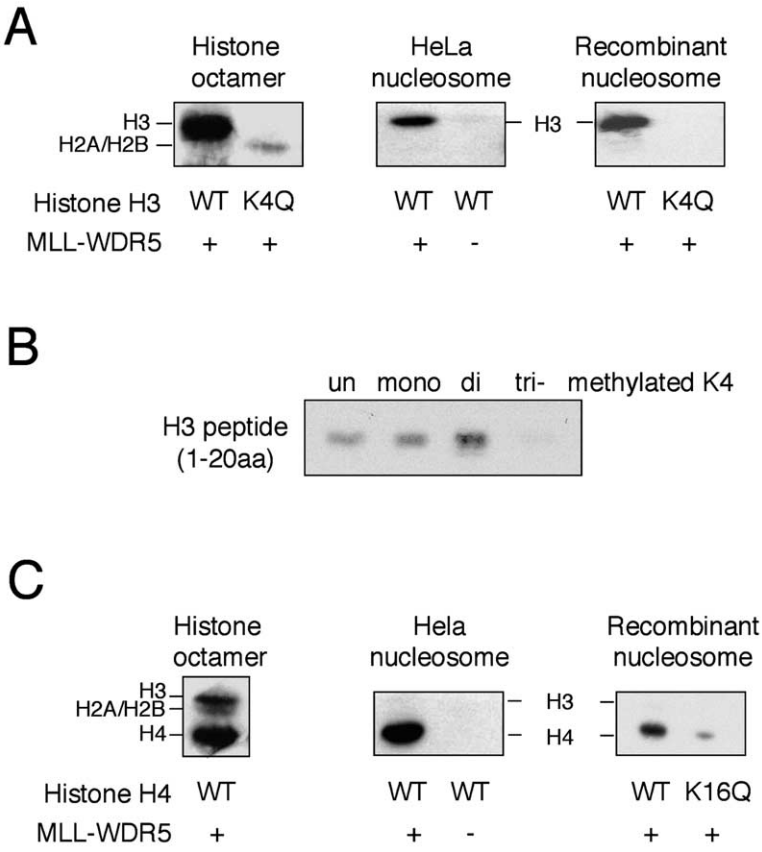

Figure 5. The MLL1-WDR5 Complex Has HMT and HAT Activities

(A) Methylation of H3 K4 by the MLL1-WDR5 complex on free histone octamers or on native or recombinant nucleosomes with wt or mutated (K4Q) H3. Addition of purified MLL1-WDR5 complex is indicated.

(B) Methylation by the MLL1-WDR5 complex of H3 peptides with different levels of K4 premethylation.

(C) Acetylation of histones on free histone octamers or nucleosomes with wt or mutated (K16Q) H4. Addition of purified MLL1-WDR5 complex is indicated.

ciently bind MLL1, MOF, and other components of the MLL1-WDR5 complex from HeLa nuclear extracts (Figure 6A). This interaction allowed us to use p53 as the activator for our in vitro transcription assay. When assayed according to the scheme in Figure 6B, p53-dependent transcription was significantly enhanced by the MLL1-WDR5 complex when added with S-adenosyl methionine (SAM; allowing methylation) or acetyl-CoA (allowing acetylation). This activation is a direct result of HMT and HAT activities of the MLL1-WDR5 complex since adding the MLL1-WDR5 complex without cofactors or adding cofactors without the MLL1-WDR5 complex had no effect (Figure 6C). Higher levels of activity that were at least equal to the sum of the individual SAM and acetyl-CoA activities were observed when SAM and acetyl-CoA were added together with the MLL1-WDR5 complex, indicating a moderate cooperativity between MLL1 and MOF (Figure 6C, lane 4). This transcription activation is activator dependent, since the transcription activity is greatly reduced in the absence of p53 (Figure 6C, lane 5). The results of several independent transcription experiments are quantified and summarized in Figure 6D. Further mechanistic analysis showed p53-dependent H3 methylation and H4 acetylation of the chromatin template by the MLL1-MOF-WDR5 complex (Figure 6E). These results are consistent with the results of the p53 interaction and transcriptional activation studies and indicate that coactivation by MLL1 and MOF involves targeted (p53-dependent) histone acetylation and methylation.

MLL1 Targets Both H3 K4 Methylation and H4 K16 Acetylation Activities to the *Hoxa9* Locus

Given the physical and functional interactions of MLL1 and MOF, we next examined H4 K16 acetylation and H3 K4 trimethylation on well-established MLL1 target genes in vivo. Three cell lines have been used: $Mll^{(+/+)}$ and $Mll^{(-/-)}$ fibroblast lines established from day 10.5 embryos and an $Mll^{(-/-)}$ + MLL1 line established by stably transfecting $Mll^{(-/-)}$ cells with a human Flag-tagged MLL1 expression construct (Milne et al., 2002). *Hoxa9* expression measured by quantitative RT-PCR showed a greater than 5-fold difference in $Mll^{(+/+)}$ cells compared with $Mll^{(-/-)}$ cells. However, ectopic expression of MLL1 in $Mll^{(-/-)}$ cells restored much of the *Hoxa9* expression (Figure 7A). To detect MLL1 binding at the *Hoxa9* locus, ChIP assays for four *Hoxa9* regions were performed (Figure 7B). These regions were located ~200–300 bp upstream of the first exon (1), within the first exon (2,3) and within second exon that contains the homeodomain (4) of *Hoxa9* (Figure 7C). Using an antibody against MLL^C in the CHIP assay, and as expected, MLL1 binding was detected in all four regions in wild-type $Mll^{(+/+)}$ cells and in $Mll^{(-/-)}$ + MLL1 cells (Figure 7D). As a control, binding at the *Gapdh* locus was at a background level similar to that seen in $Mll^{(-/-)}$ cells. Consistent with the binding of MLL1 to the *Hoxa9* locus, changes of H3 K4 dimethylation and trimethylation tightly correlated with MLL1 binding to this locus (regions 1-4). Fold differences between the di- and trimethylation levels of H3 K4 in $Mll^{(+/+)}$ and $Mll^{(-/-)}$ +

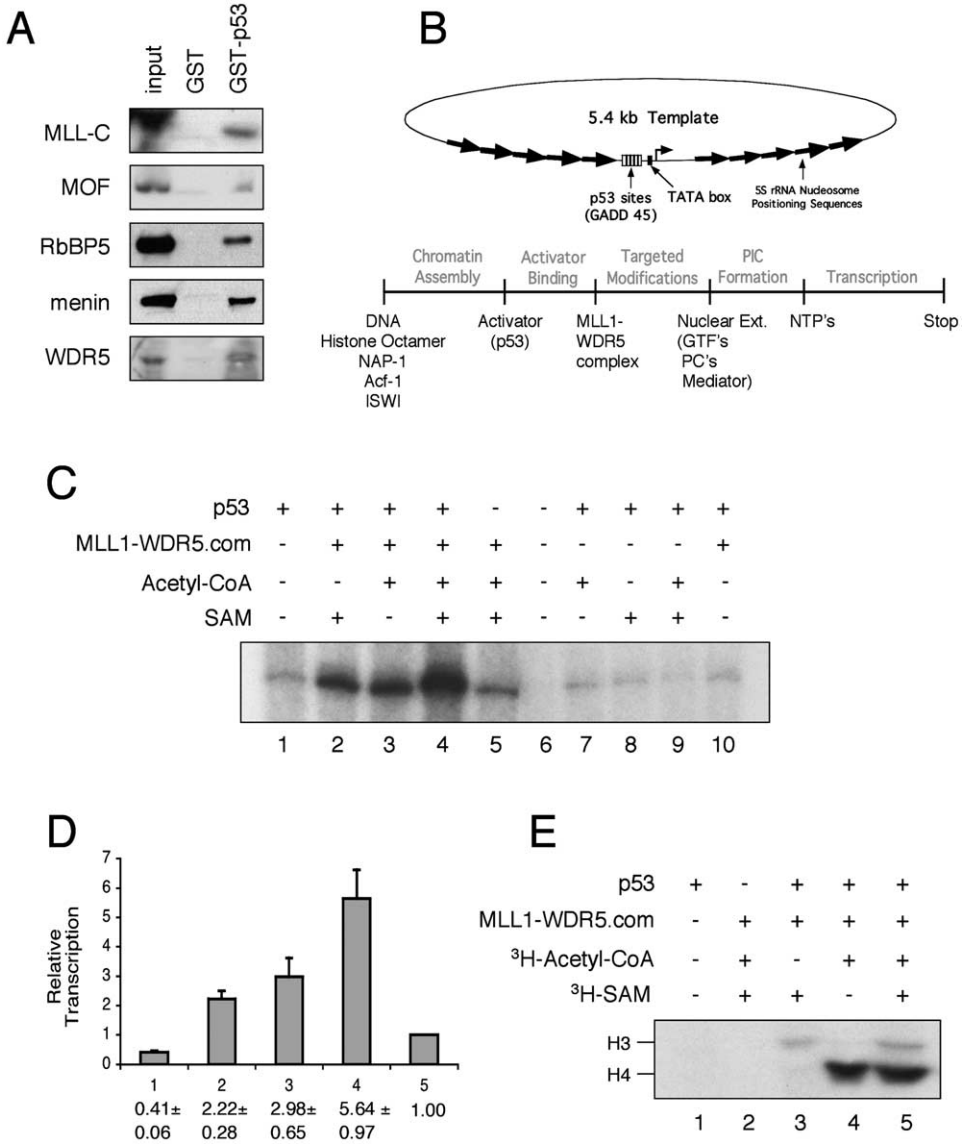

Figure 6. The HMT and HAT Activities of the MLL1-MOF Complex Modify Histones in an Activator-Dependent Manner and Act Coordinately to Effect p53-Dependent Transcription on Chromatin

(A) Binding of the MLL1-WDR5 complex (from nuclear extract) to GST-p53. Bound proteins (indicated at left) were analyzed by immunoblot.

(B) Schematic of in vitro transcription assay using recombinant chromatin templates (An and Roeder, 2004).

(C) Chromatin-templated transcription assays with p53, purified MLL1-WDR5 complex, acetyl-CoA, and SAM addition as indicated and according to the scheme in (B).

(D) Quantitation by phosphoimager of data as in (C) (lanes 1–5) is shown. y axis indicates transcription levels relative to lane 5 (p53-independent basal activity). Average and standard deviations (error bars) from three autoradiographic analyses are indicated at the bottom.

(E) Histone modification assays on chromatin templates with p53, purified MLL1-WDR5 complex, acetyl-CoA, and SAM additions as indicated.

MLL1 cells compared with that in *Mll*$^{(-/-)}$ cells are shown in Figures 7E and 7F. As a control, no change in di- or trimethylation was seen at the *Gapdh* locus, which does not have bound MLL1.

We next examined H4 acetylation using antibodies against specific lysine residues, namely K5, K8, K12, and K16, across the *Hoxa9* locus in the three cell lines. These four acetylation sites showed very different responses in relation to bound MLL1. There was no change in K5 acetylation and only small increases in K8 and K12 acetylation at the *Hoxa9* locus in *Mll*$^{(+/+)}$ cells and in *Mll*$^{(-/-)}$ + MLL1 cells when compared with *Mll*$^{(-/-)}$ cells (Figures 7G, 7H, and 7I). In contrast, the K16 acetylation level increased dramatically across the *Hoxa9* locus in both *Mll*$^{(+/+)}$ and *Mll*$^{(-/-)}$ + MLL1 cells (Figure 7J). Comparing the changes in H3 K4 methylation and in H4 K16 acetylation within the *Hoxa9* locus, a close correlation of these two marks was also observed. There was gradual increase of H3 K4 methylation from regions 1 to 4, and a similar pattern was de-

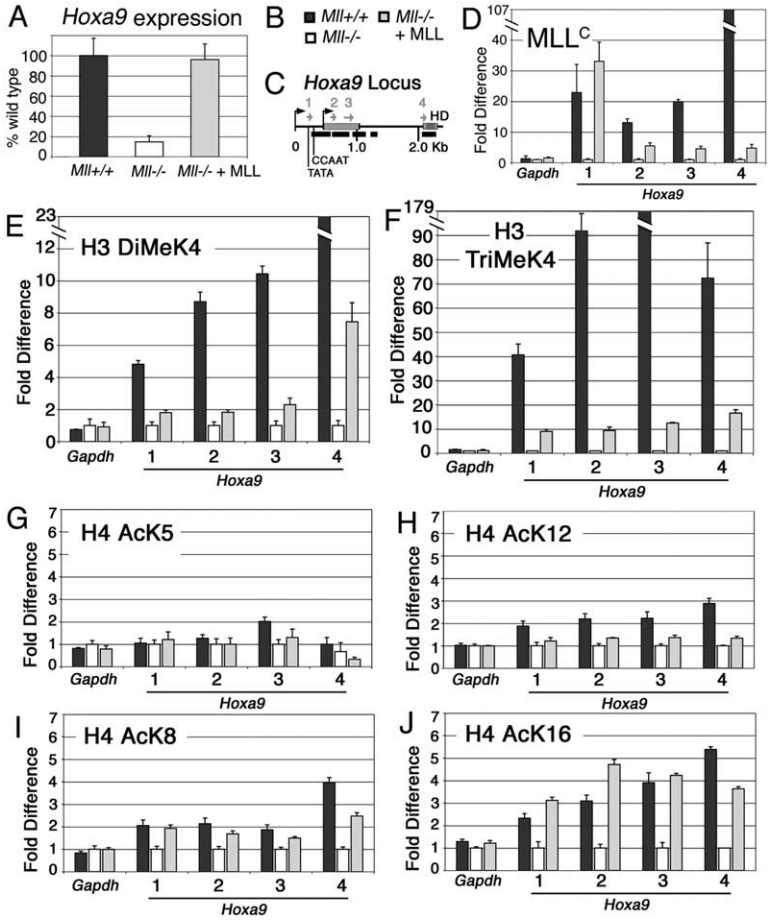

Figure 7. Specific Increase of H4 K16 Acetylation upon MLL1 Binding at the *Hoxa9* Promoter

(A) Reduced *Hoxa9* expression in *Mll*$^{(-/-)}$ cells and restoration by ectopic MLL1. *Hoxa9* expression in wt cells (dark gray) is arbitrarily set as 100%. Standard deviations in this and other experiments (D–J) are indicated by error bars.

(B) Legend for (D)–(H). Dark gray, *Mll*$^{(+/+)}$ cells; white, *Mll*$^{(-/-)}$ cells; light gray, *Mll*$^{(-/-)}$ + ectopic MLL1-expressing cells.

(C) Four probe sets in the *Hoxa9* locus used for real-time PCR quantification of ChIP. Black bars indicate CpG-rich regions of the locus; arrows indicate two different transcription start sites (Fujimoto et al., 1998); putative TATA boxes are shown (Nakamura et al., 2002), and the first and second exons are shown as gray boxes. The homeodomain (HD) in exon 2 is indicated by crosshatching.

(D–J) ChIP experiments in *Mll*$^{(+/+)}$, *Mll*$^{(-/-)}$, and *Mll*$^{(-/-)}$ + MLL1 cells using the indicated antibodies. ChIP was quantified using the Taqman primer/probe sets indicated in (C). Signals in *Mll*$^{(-/-)}$ cells were set to 1, and signals in *Mll*$^{(+/+)}$ and *Mll*$^{(-/-)}$ + MLL1 cells were expressed as fold differences relative to *Mll*$^{(-/-)}$ cells. (D) MLL^{C}, (E) H3 di-MeK4, (F) H3 tri-MeK4, (G) H4 AcK5, (H) H4 AcK12, (I) H4 AcK8, (J) H4 AcK16.

tected for H4 K16 acetylation. Since, in all cases, we scored the fold difference in histone modifications at the *Hoxa9* locus in *Mll*$^{(+/+)}$ and *Mll*$^{(-/-)}$ + MLL1 cells to that in *Mll*$^{(-/-)}$ cells, the changes in K4 methylation and H4 K16 acetylation reported here are MLL1 dependent. No MLL1-dependent changes in H3 K4 methylation or H4 K16 acetylation were seen at the *Gapdh* locus, which is not regulated by MLL1, suggesting that changes observed at the *Hoxa9* locus require MLL1 binding. Thus, these analyses have established a clear correlation between H3 K4 methylation and H4 K16 acetylation at the *Hoxa9* locus and, most significantly, a strong dependence of the H4 K16 acetylation on the presence of MLL1.

MOF Is Required for the Expression of *HOXA9*

The in vivo function of MOF on the well-established MLL1 target gene *HOXA9* was further explored in HeLa cells. MOF expression was effectively eliminated by siRNA techniques (Figure 8A). As revealed by immunoblot using acetylated H3 as an internal control, MOF siRNA resulted in a significant reduction of the global H4 K16 acetylation level (~30%) relative to that observed with control siRNA-treated cells. This indicates that MOF is the major histone acetyltransferase for this site in vivo. Quantitative real time RT-PCR analysis further showed that *HOXA9* expression was significantly downregulated (>50% decrease) in the MOF knockdown cells compared to control siRNA-treated cells (Figure 8B). The expression of *GAPDH*, which is not an MLL1 target, was less affected (inconsistent small reductions were observed in some cases) by MOF siRNA treatment. In all cases, *HOXA9* and *GAPDH* expression levels were normalized to total input RNA.

To detect H4 K16 acetylation and H3 K4 methylation at the *HOXA9* locus, ChIP assays were directed toward a *HOXA9* TATA-containing region (1) located ~200–300 bp upstream of the first exon and a region (3) within the first exon (Figure 7C). MOF knockdown resulted in a significant reduction of H4 K16 acetylation both around the TATA region (~50% decrease) and in the coding region (~70% decrease). Consistent with the expression results, the K16 acetylation level on *GAPDH* was less (and inconsistently) affected by MOF siRNA. No significant changes in trimethylation at the *HOXA9* locus were observed in MOF siRNA-treated cells (Figure 8D). This indicates that whereas H4 K16 acetylation by MOF is dependent upon MLL1 (Figure 7), H3 K4 methylation by MLL1 can occur independently of MOF. Considering that MOF stably associates with MLL1, that MLL1 and MOF coordinately activate transcription in vitro, and that K16 acetylation at the *HOXA9* locus is

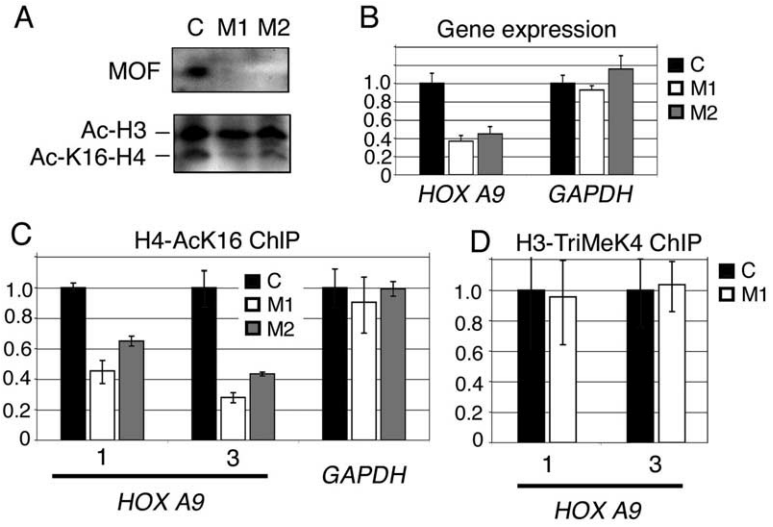

Figure 8. Loss of MOF Protein Results in a Decrease of Histone H4 Lysine 16 Acetylation and *HOXA9* Expression

(A) MOF siRNAs, M1 and M2, decrease MOF protein and global H4 K16 acetylation levels. Acetylated H3 was used as internal loading control.

(B) MOF siRNA treatment reduces *HOXA9* gene expression. Expression levels of *HOXA9* and *GAPDH* in MOF siRNA-treated cells (M1 and M2) are normalized to levels in control cells (C). Standard deviations in (B)–(C) are indicated by error bars.

(C) Histone H4 K16 acetylation at *HOXA9* and *GAPDH* loci in MOF (M1 and M2) and control (C) siRNA-treated cells. The K16 acetylation level in MOF siRNA-treated cells is normalized to the level in control cells (C), which is arbitrarily set as 1.

(D) Histone H3 K4 methylation at the *HOXA9* locus in MOF (M1) and control (C) siRNA-treated cells. H3 K4 methylation in control cells (C) is arbitrarily set as 1.

MLL1 dependent, it is highly probable that downregulation of *HOXA9* by MOF siRNA treatment is specific and direct.

Discussion

Studies to date indicate that the chromatin modifications associated with gene activation are diverse and involve the action of combinations of histone modifying enzymes/coactivators (Fischle et al., 2003; Turner, 2002). In studies directed toward the function of human MLL1 in transcription activation through H3 K4 methylation, we have identified a stable complex (MLL1-WDR5) containing both MLL1 and the MYST family histone acetyltransferase MOF. The relevance of the demonstrated ability of this complex to effect both H3 K4 methylation (mono-, di-, tri-) and H4 K16 acetylation, to interact with a transcriptional activator, and to stimulate activator-dependent transcription through the resident HMT and HAT activities in vitro is underscored by our concomitant demonstration of MLL1-dependent H3 K4 methylation and H4 K16 acetylation events on a known MLL1 target gene. Altogether, these results indicate a coordinate function of MLL1 and MOF, through a physical association, in gene activation events. Along with complementary studies (Wysocka et. al., 2005 [this issue of *Cell*]) indicating direct interactions of WDR5, an MLL1-interacting component of the MLL1-MOF complex, with methylated H3 K4 residues, these results also lead to a model for both the establishment and spreading of K4 methylation, perhaps in conjunction with H4 K16 acetylation, in transcriptionally active chromatin.

MLL1 and MOF Can Form a Stable Complex In Vivo

The MLL1-WDR5 complex purified on the basis of an intrinsic epitope-tagged subunit (WDR5) represents a unique subpopulation of cellular MLL1 complexes with novel components (notably MOF; see Table S1 in the Supplemental Data available with this article online). This idea is supported by our observation of two MLL1-containing peaks following the fractionation of nuclear extract by gel filtration (data not shown) and by previous indications of heterogeneity in the MLL1-HCF preparation (Yokoyama et al., 2004).

That MOF is a bona fide component of an MLL1-containing complex is indicated by (1) copurification through ion-exchange chromatography and affinity purification steps (involving epitope-tagged WDR5 or RbBP5), (2) cosedimentation on sucrose gradients of MOF with MLL1 and other core components (WDR5, Ash2L, RbBP5) of the purified MLL1-WDR5 complex, (3) coimmunoprecipitation of MLL1 and select components (including Ash2L, RbBP5, Ring2, and WDR5) of the MLL1-WDR5 preparation using anti-MOF antibody, (4) coimmunoprecipitation of MLL1, MOF, and Ring2 following pairwise expression in transfected cells, and (5) direct in vitro interactions between MLL1 and MOF, through mapped subdomains. The possibility that MOF might also be associated with contaminating hSET1 and MLL2 complexes, which also contain WDR5, is ruled out by the failure of anti-MOF antibodies to coimmunoprecipitate the residual amounts of hSET1 or MLL2 in the MLL1-WDR5 preparation and by MOF coimmunoprecipitation with f-RbBP5 (which is not a component of the hSET1 complex). This is consistent with the greater abundance of MOF (detected by mass spectrometry) relative to hSET1 or MLL2 (not detected by mass spectrometry) in the MLL1-WDR5 preparation.

Although well-studied in *Drosophila*, very little is known about MOF in mammalian cells. The *Drosophila* ortholog (dMOF) of human MOF is important for dosage compensation of the male X chromosome and acts through an H4 K16 acetylation mechanism that effects a 2-fold activation of transcription (Smith et al., 2000). In *Drosophila*, dMOF function in dosage compensation depends on its integration into a complex with male-specific MSL1, MSL2, and other components (Morales et al., 2004). It has been suggested that a similar dosage compensation complex also exists in mammals

(Neal et al., 2000), but its function remains enigmatic since mammals use a totally different mechanism for dosage compensation. The presence in the MLL1-WDR5 complex of MOF suggests that, in mammals, MOF probably plays an alternative role in transcription regulation that is independent of the dosage compensation system.

The MLL1-WDR5 Complex Is Enzymatically Active

Although lysine residues may be mono-, di-, or trimethylated in vivo, the trimethyl H3 K4 is preferentially and strongly associated with the transcribed regions of active genes from yeast to higher eukaryotes (Krogan et al., 2002; Ng et al., 2003; Santos-Rosa et al., 2002; Schneider et al., 2004). In yeast, SET1 is the only H3 K4 methyltransferase and can methylate H3 K4 to all three levels. In contrast, higher eukaryotes contain several H3 K4 methyltransferases with various specificities, suggesting a more complex picture for the regulation and function of H3 K4 methylation in higher eukaryotes (Sims et al., 2003).

The purified MLL1-WDR5 complex shows a robust H3 K4 methyltransferase activity on H3 peptide, free histone octamer, and nucleosomal substrates. Importantly, like SET1 in yeast, the MLL1-WDR5 complex is active with non-, mono-, and dimethylated substrates and, in particular, efficiently converts dimethylated H3 K4 residues (the preferred substrate) to trimethylated residues. This result is consistent with the view that MLL1 is directly involved in transcription activation of *Hox* genes as a consequence of the enhanced levels of H3 K4 trimethylation associated with MLL1 binding to *Hox* gene promoters in vivo. This result contrasts with the reported inability of the MLL1 supercomplex (weak HMT activity) or the MLL1 SET domain (much stronger HMT activity) to effect H3 K4 trimethylation. Thus, and consistent with its distinct composition relative to that of the first reported MLL1 complex (Nakamura et al., 2002), the MLL1-WDR5 complex described here is more likely to be the functionally active MLL1 complex. Since a recombinant MLL^{C} fragment (180 kDa) shows extremely weak activity compared with the MLL1-WDR5 complex (data not shown), it appears that MLL1, like yeast SET1, must be associated with other components for full activity. With respect to the MLL1-associated HAT activity of MOF, *Drosophila* MOF has an unusually narrow substrate specificity and only acetylates histone H4 K16 on a nucleosomal template (Akhtar and Becker, 2000; Smith et al., 2000). Moreover, faithful and efficient acetylation of nucleosomal histone H4 by MOF is observed only upon interaction with MSL1 and MSL3 (Morales et al., 2004). MOF in the MLL1-WDR5 complex shows a similar preference for H4 K16 on nucleosomes. In fact, the observed reduction of global H4 K16 acetylation in MOF knockdown cells suggests that MOF is one of the major histone acetyltransferases involved in H4 K16 acetylation and may play important roles in functions other than dosage compensation.

Analysis of the MOF and MLL1 interaction domains has further shown that MLL1, via a C-terminal domain, interacts with the zinc finger of MOF. Given that an interaction of dMOF with MSL1 through its zinc finger is essential for correct targeting of MOF to the male X chromosome (Morales et al., 2004), analogous interactions of hMOF with MLL1 through the same zinc finger region may imply new functions for MOF, possibly by targeting different sets of genes through its interaction with MLL1-WDR5.

HMT and HAT Activities of the MLL1-WDR5 Complex Can Act Coordinately in Transcriptional Regulation

The use of a chromatin-templated assay in which transcription is dependent upon a transcriptional activator and interacting chromatin modifying cofactors has allowed us to document in vitro functions of the MLL1 HMT and MOF HAT activities. Thus, in the absence of other factors (p300, CARM1, PRMT1) previously shown to serve as coactivators in this assay (An et al., 2004), p53-mediated transcription is dependent upon addition of the MLL1-MOF-WDR5 complex and either SAM or acetyl-CoA. The dependence on these cofactors indicates that the coactivator functions can be attributed to the histone methyltransferase and histone acetyltransferase activities of MLL1 and MOF, respectively. The inability of p53 to enhance transcription upon addition of SAM and acetyl-CoA without the MLL1-WDR5 complex indicates that the observed activation by p53 is not due to endogenous MLL1 or MOF. Reciprocally, the lack of an effect of the MLL1-WDR5 complex (with SAM and acetyl-CoA) in the absence of p53 indicates that transcription activation does not result from general (nontargeted) modifications of the chromatin template. This is further indicated by our demonstration of p53-dependent (targeted) methylation and acetylation of chromatin template histones by MLL1 and MOF. The fact that histone modifications by the MLL1-MOF-WDR5 complex are p53 dependent and correlate with transcriptional activation indicates a direct involvement of MLL1 and MOF in p53-dependent transcription. This is consistent with our demonstrated interaction of the MLL1-WDR5 complex with p53, as well as prior indications of p53-induced accumulation of methylated H3 K4 on a p53 target gene (An et al., 2004). The possible involvement of the MLL1-WDR5 complex in transcription initiation is consistent with the reported enrichment of di- and trimethylated H3 K4 at active promoters in higher eukaryotes (Santos-Rosa et al., 2002; Schneider et al., 2004) and is further supported by studies indicating enhanced transcription of a reporter with Gal4 binding sites following expression (and artificial recruitment) of a Gal4-WDR5 fusion protein (Wysocka et al., 2005).

The coordinate action of MLL1 HMT and MOF HAT activities in the in vitro assays is in agreement with the close correlation between H3 K4 methylation and histone acetylation marks in vivo but describes cooperation that is site specific and involves only H3 K4 and H4 K16. In contrast to other acetylated residues on H4, acetylated K16 is known to play a pivotal role in determining the potential of coding DNA for expression or silencing. Thus, (1) only the H4 K16 mutation has specific transcription consequences independent of the mutational state of the other lysines (Dion et al., 2005), (2) in yeast, H4 K16 is the only residue whose acetylation can, on its own, prevent silencing of the mating type genes (Johnson et al., 1990; Megee et al., 1990), and (3) MOF can activate transcription in yeast when

tethered to a promoter via a DNA binding domain, suggesting that a rather local acetylation may lead to a significant stimulation of transcription (Akhtar and Becker, 2000). The potentially cooperative in vivo functions between H3 K4 methylation and H4 K16 acetylation have clearly been demonstrated by the downregulation of a well-established MLL1 target gene, *Hoxa9*, in MOF siRNA-treated cells and by a specific increase in H4 K16 acetylation, which is dependent on MLL1 and closely correlated with the MLL1-dependent increase in H3 K4 methylation, in the same locus. Our hypothesis of coordinate MLL1 and MOF function is further supported by our demonstration that MOF, like other (e.g., RbBP5) components of MLL1-WDR5 complex, can bind to methylated H3 K4 through WDR5, arguing for the joint recruitment of HMT and HAT activities to the same targets (Figure S2).

Model for Transcription Activation

Our demonstration of transcriptional activation through the HMT (MLL1) and HAT (MOF) activities in the MLL1-WDR5 complex, direct interaction of the complex with a DNA binding transcriptional activator, and binding of a resident subunit (WDR5) to methylated H3 K4 (Wysocka et al., 2005) lead to a model for both the establishment and spreading of an active chromatin structure. The model invokes activator binding to DNA regulatory elements, activator-mediated recruitment of the MLL1-WDR5 complex, consequent methylation and acetylation, and either the recruitment of additional MLL1-WDR5 complexes or internucleosomal transfer of primary MLL1-WDR5 complexes through binding of the WDR5 subunit to methylated H3 K4 or through binding of the MLL1 bromodomain to acetylated H4 K16 residue. This model is related, in part, to that proposed for propagation of heterochromatin by H3 K9 methylation and subsequent HP1 binding (Lachner et al., 2001).

Previously established H3 K4 methylation marks can also be recognized by other effectors, such as CHD1 in the SAGA complex (Pray-Grant et al., 2005) and components in ATP-dependent chromatin remodeling complexes (Beisel et al., 2002; Santos-Rosa et al., 2003). Similarly, acetylation marks can also be recognized by various bromodomains (Hassan et al., 2001) that are common structural features of many histone acetyltransferases (Turner, 2002). Recruitment of other HAT complexes and ATP-remodeling complexes by molecules that directly or indirectly interact with methyl- or acetylmarks may further facilitate the spreading of "open chromatin" and enable RNA polymerase to efficiently move through the chromatin template for active transcription.

Experimental Procedures

Cell Lines

$Mll^{(+/+)}$, $Mll^{(-/-)}$, and $Mll^{(-/-)}$ + MLL cell lines have been described previously (Milne et al., 2002). The f-WDR5 and f-RbBP5 cell lines were made by transfecting HeLa S3 cells with either an f-WDR5-pIRESneo vector or an f-RbBP5-pIRESneo vector.

Fractionation of Nuclear Extracts

Nuclear extracts were obtained from f-WDR5 or f-RbBP5 cells by a modified Dignam procedure (Dignam et al., 1983) and fractionated according to the scheme in Figure 1A. For sucrose gradient sedimentation, 500 μl purified MLL1-WDR5 complex (from 50 ml nuclear extract) was loaded onto an 11 ml 10% to 40% (w/v) sucrose gradient. After centrifugation for 16 hr at 23,000 rpm (SW41 rotor), 0.5 ml fractions were collected.

Immunoaffinity Purification of the MLL1-WDR5 Complex and Mass Spectrometry

The SP Sepharose BC500 fraction was incubated with M2 agarose in BC300, 0.05%NP40 at 4°C for 4 hr and extensively washed with BC500, 0.05% NP40. The complex was eluted with 0.25 mg/ml Flag peptide in BC100. The eluted MLL1-WDR5 complex was resolved by SDS-PAGE and visualized by zinc staining. The entire gel lane was sliced into 2 mm bands and proteins were subjected to MALDI mass spectrometry (Krutchinsky et al., 2000; Krutchinsky et al., 2001). Proteins were identified by XProteo (Chao Zhang; http://www.xproteo.com). Common background proteins (i.e., keratins, tubulins, ribosomal proteins) were excluded from the list of interacting proteins. We also note that WDR5-Flag was identified in multiple bands, which may be due to breakdown and/or overloading.

Antibodies

Anti-MLL^C antibody was generated using the previously described epitope (Hsieh et al., 2003). Other antibodies were obtained commercially as follows: anti-MLL-N, hSET1, MLL2, menin, RbBP5, and Ash2 (Bethyl Laboratory); anti-TIP60 (Santa Cruz); mouse IgG, M2, and M2 agarose (Sigma); anti-His (Qiagen); anti-HA (Roche); anti-H3 dimethyl K4 and trimethyl K4 (Abcam); anti-H4 acetyl K5, acetyl K8, acetyl K12, and acetyl K16 (Upstate Biotechnology). Anti-MOF and anti-MSL1 antibodies will be described elsewhere (E.R.S., C. Cayrou, R. Huang, W.S. Lane, J. Cote, and J.C. Lucchesi, unpublished data).

Plasmids and Expression Vectors

Bacterial vectors for core histone expression and purification were as described (Luger et al., 1999). Mutations (H3 K4 and H4 K16) were introduced by PCR-based site-directed mutagenesis. Flag-tagged p53 and the DNA template for transcription were as described (An et al., 2004). GST and GST-tagged WDR5, RbBP5, MOF full length, MOF (1–171), and MOF (1–235) proteins were expressed in bacteria from the pGEX4T-1 vector (Amersham). A Flag-tagged MLL^C cDNA was inserted into pVL1392 baculovirus vector (Bacvector 3000, Novagen). For transfection assays, cDNAs encoding tagged MLL1, MOF, and Ring2 proteins were inserted into the CMV-driven expression vector pIRESneo (Clontech). Manufacturer's protocols for the TNT Quick coupled transcription/translation system (Promega) were used for in vitro translation. Information for in vitro translation templates is in the Supplemental Data.

GST Pull-Down Assay

For GST pull-down assays, 4 μg GST-tagged protein and 200 μl HeLa NE, 10 μl of the TNT translation reaction or 2 μg purified recombinant MLL^C were used in each binding assay. Reactions were carried out at 4°C for 4 hr and beads were washed three times with BC200.

Histone Modification Assays

Unmodified, mono-, di-, and trimethylated H3 K4 peptides were from Upstate Biotechnology. HeLa nucleosomes were purified as described (Owen-Hughes et al., 1999). Recombinant nucleosomes were prepared by salt dialysis using 5S array DNA from G5ML (Kundu et al., 2000) and recombinant histone octamers were reconstituted as described (Luger et al., 1999). For each HMT or HAT assay, 5 μg peptide, 2 μg HeLa nucleosomes, or 2 μg recombinant nucleosomes were used. Reactions were carried out at 30°C for 1 hr in the presence of [^{3}H]-SAM (S-adenosyl-L-[methyl-^{3}H] methionine) or [^{3}H]-acetyl-CoA.

Chromatin Modifications and Transcription Assays

Chromatin assembly and histone modification reactions were carried out with coactivators essentially as described (An and Roeder,

2004). Transcription assays included 40 ng p53 and about 100 ng purified MLL1-WDR5 for each reaction.

Chromatin Immunoprecipitation (ChIP) and Q-PCR Reactions

Chromatin immunoprecipitations were performed using the Chromatin Immunoprecipitation Assay Kit (Upstate, Lake Placid, New York) and protocols recommended by the manufacturer. Real-time PCR quantitation of ChIP was performed in triplicate using Taqman probes and an ABI Prism 7700 (Applied Biosystems) and both the relative quantification and percent input methods as outlined in Milne et al. (2002). Real-time PCR quantitations of *Hoxa9* and *Gapdh* expression in MOF siRNA experiments were normalized against input total RNA.

RNA Interference

HeLa cells were transfected with siRNA duplexes (200 pmol; Dharmacon) using Oligofectamine (Invitrogen) according to the manufacturer's instructions. One additional round of transfection was performed under identical conditions 48 hr after the initial transfection. Cells were harvested 48 hr after the second transfection. The sequences for MOF small interfering RNAs (siRNAs) used in the assays are available upon request.

Supplemental Data

Supplemental Data include two figures, one table, and Supplemental Experimental Procedures and can be found with this article online at http://www.cell.com/cgi/content/full/121/6/873/DC1/.

Acknowledgments

We are grateful to Drs. S. Korsmeyer, W. Herr, T. Tamura, and M. Vidal for antibodies and J. Kim and Drs. Q. Yang and S. Malik in the Roeder lab for technical advice. Y.D. is a fellow of the Irvington Institute for Immunological Research; J.W. is a fellow of the Damon Runyon Cancer Research Foundation, and A.F. is a fellow of the Japan Society for the Promotion of Science. This work was supported by NIH grants (to J.L.H., B.T.C., A.J.T., and C.D.A), by a Leukemia and Lymphoma Society of America SCOR grant (to J.L.H.), and by funds from the Rockefeller University (to R.G.R.).

Received: January 26, 2005
Revised: March 25, 2005
Accepted: April 28, 2005
Published: June 16, 2005

References

Akhtar, A., and Becker, P.B. (2000). Activation of transcription through histone H4 acetylation by MOF, an acetyltransferase essential for dosage compensation in *Drosophila*. Mol. Cell *5*, 367–375.

An, W., and Roeder, R.G. (2004). Reconstitution and transcriptional analysis of chromatin *in vitro*. Methods Enzymol. *377*, 460–474.

An, W., Palhan, V.B., Karymov, M.A., Leuba, S.H., and Roeder, R.G. (2002). Selective requirements for histone H3 and H4 N termini in p300-dependent transcriptional activation from chromatin. Mol. Cell *9*, 811–821.

An, W., Kim, J., and Roeder, R.G. (2004). Ordered cooperative functions of PRMT1, p300, and CARM1 in transcriptional activation by p53. Cell *117*, 735–748.

Beisel, C., Imhof, A., Greene, J., Kremmer, E., and Sauer, F. (2002). Histone methylation by the Drosophila epigenetic transcriptional regulator Ash1. Nature *419*, 857–862.

Carrozza, M.J., Utley, R.T., Workman, J.L., and Cote, J. (2003). The diverse functions of histone acetyltransferase complexes. Trends Genet. *19*, 321–329.

Corona, D.F., Clapier, C.R., Becker, P.B., and Tamkun, J.W. (2002). Modulation of ISWI function by site-specific histone acetylation. EMBO Rep. *3*, 242–247.

Dignam, J.D., Lebovitz, R.M., and Roeder, R.G. (1983). Accurate transcription initiation by RNA polymerase II in a soluble extract from isolated mammalian nuclei. Nucleic Acids Res. *11*, 1475–1489.

Dion, M.F., Altschuler, S.J., Wu, L.F., and Rando, O.J. (2005). From the cover: genomic characterization reveals a simple histone H4 acetylation code. Proc. Natl. Acad. Sci. USA *102*, 5501–5506.

Ernst, P., Wang, J., Huang, M., Goodman, R.H., and Korsmeyer, S.J. (2001). MLL and CREB bind cooperatively to the nuclear coactivator CREB-binding protein. Mol. Cell. Biol. *21*, 2249–2258.

Fischle, W., Wang, Y., and Allis, C.D. (2003). Histone and chromatin cross-talk. Curr. Opin. Cell Biol. *15*, 172–183.

Fujimoto, S., Araki, K., Chisaka, O., Araki, M., Takagi, K., and Yamamura, K. (1998). Analysis of the murine Hoxa-9 cDNA: an alternatively spliced transcript encodes a truncated protein lacking the homeodomain. Gene *209*, 77–85.

Goo, Y.H., Sohn, Y.C., Kim, D.H., Kim, S.W., Kang, M.J., Jung, D.J., Kwak, E., Barlev, N.A., Berger, S.L., Chow, V.T., et al. (2003). Activating signal cointegrator 2 belongs to a novel steady-state complex that contains a subset of trithorax group proteins. Mol. Cell. Biol. *23*, 140–149.

Hassan, A.H., Neely, K.E., and Workman, J.L. (2001). Histone acetyltransferase complexes stabilize SWI/SNF binding to promoter nucleosomes. Cell *104*, 817–827.

Hess, J.L. (2004). MLL: a histone methyltransferase disrupted in leukemia. Trends Mol. Med. *10*, 500–507.

Hsieh, J.J., Ernst, P., Erdjument-Bromage, H., Tempst, P., and Korsmeyer, S.J. (2003). Proteolytic cleavage of MLL generates a complex of N- and C-terminal fragments that confers protein stability and subnuclear localization. Mol. Cell. Biol. *23*, 186–194.

Hughes, C.M., Rozenblatt-Rosen, O., Milne, T.A., Copeland, T.D., Levine, S.S., Lee, J.C., Hayes, D.N., Shanmugam, K.S., Bhattacharjee, A., Biondi, C.A., et al. (2004). Menin associates with a trithorax family histone methyltransferase complex and with the hoxc8 locus. Mol. Cell *13*, 587–597.

Johnson, L.M., Kayne, P.S., Kahn, E.S., and Grunstein, M. (1990). Genetic evidence for an interaction between SIR3 and histone H4 in the repression of the silent mating loci in *Saccharomyces cerevisiae*. Proc. Natl. Acad. Sci. USA *87*, 6286–6290.

Krogan, N.J., Dover, J., Khorrami, S., Greenblatt, J.F., Schneider, J., Johnston, M., and Shilatifard, A. (2002). COMPASS, a histone H3 (Lysine 4) methyltransferase required for telomeric silencing of gene expression. J. Biol. Chem. *277*, 10753–10755.

Krutchinsky, A.N., Zhang, W., and Chait, B.T. (2000). Rapidly switchable matrix-assisted laser desorption/ionization and electrospray quadrupole-time-of-flight mass spectrometry for protein identification. J. Am. Soc. Mass Spectrom. *11*, 493–504.

Krutchinsky, A.N., Kalkum, M., and Chait, B.T. (2001). Automatic identification of proteins with a MALDI-quadrupole ion trap mass spectrometer. Anal. Chem. *73*, 5066–5077.

Kundu, T.K., Palhan, V.B., Wang, Z.X., An, W.J., Cole, P.A., and Roeder, R.G. (2000). Activator-dependent transcription from chromatin in vitro involving targeted histone acetylation by p300. Mol. Cell *6*, 551–561.

Lachner, M., O'Carroll, N., Rea, S., Mechtler, K., and Jenuwein, T. (2001). Methylation of histone H3 lysine 9 creates a binding site for HP1 proteins. Nature *410*, 116–120.

Luger, K., Rechsteiner, T.J., and Richmond, T.J. (1999). Preparation of nucleosome core particle from recombinant histones. Methods Enzymol. *304*, 3–19.

Megee, P.C., Morgan, B.A., Mittman, B.A., and Smith, M.M. (1990). Genetic analysis of histone H4: essential role of lysines subject to reversible acetylation. Science *247*, 841–845.

Milne, T.A., Briggs, S.D., Brock, H.W., Martin, M.E., Gibbs, D., Allis, C.D., and Hess, J.L. (2002). MLL targets SET domain methyltransferase activity to Hox gene promoters. Mol. Cell *10*, 1107–1117.

Milne, T.A., Hughes, C.M., Lloyd, R., Yang, Z., Rozenblatt-Rosen, O., Dou, Y., Schnepp, R.W., Krankel, C., Livolsi, V.A., Gibbs, D., et al. (2005). Menin and MLL cooperatively regulate expression of cyclin-

dependent kinase inhibitors. Proc. Natl. Acad. Sci. USA *102*, 749–754.

Morales, V., Straub, T., Neumann, M.F., Mengus, G., Akhtar, A., and Becker, P.B. (2004). Functional integration of the histone acetyltransferase MOF into the dosage compensation complex. EMBO J. *23*, 2258–2268.

Nakamura, T., Mori, T., Tada, S., Krajewski, W., Rozovskaia, T., Wassell, R., Dubois, G., Mazo, A., Croce, C.M., and Canaani, E. (2002). ALL-1 is a histone methyltransferase that assembles a supercomplex of proteins involved in transcriptional regulation. Mol. Cell *10*, 1119–1128.

Neal, K.C., Pannuti, A., Smith, E.R., and Lucchesi, J.C. (2000). A new human member of the MYST family of histone acetyl transferases with high sequence similarity to Drosophila MOF. Biochim. Biophys. Acta *1490*, 170–174.

Ng, H.H., Robert, F., Young, R.A., and Struhl, K. (2003). Targeted recruitment of Set1 histone methylase by elongating Pol II provides a localized mark and memory of recent transcriptional activity. Mol. Cell *11*, 709–719.

Owen-Hughes, T., Utley, R.T., Steger, D.J., West, J.M., John, S., Cote, J., Havas, K.M., and Workman, J.L. (1999). Analysis of nucleosome disruption by ATP-driven chromatin remodeling complexes. Methods Mol. Biol. *119*, 319–331.

Petruk, S., Sedkov, Y., Smith, S., Tillib, S., Kraevski, V., Nakamura, T., Canaani, E., Croce, C.M., and Mazo, A. (2001). Trithorax and dCBP acting in a complex to maintain expression of a homeotic gene. Science *294*, 1331–1334.

Pray-Grant, M.G., Daniel, J.A., Schieltz, D., Yates, J.R., 3rd, and Grant, P.A. (2005). Chd1 chromodomain links histone H3 methylation with SAGA- and SLIK-dependent acetylation. Nature *433*, 434–438.

Santos-Rosa, H., Schneider, R., Bannister, A.J., Sherriff, J., Bernstein, B.E., Emre, N.C., Schreiber, S.L., Mellor, J., and Kouzarides, T. (2002). Active genes are tri-methylated at K4 of histone H3. Nature *419*, 407–411.

Santos-Rosa, H., Schneider, R., Bernstein, B.E., Karabetsou, N., Morillon, A., Weise, C., Schreiber, S.L., Mellor, J., and Kouzarides, T. (2003). Methylation of histone H3 K4 mediates association of the Isw1p ATPase with chromatin. Mol. Cell *12*, 1325–1332.

Schneider, R., Bannister, A.J., Myers, F.A., Thorne, A.W., Crane-Robinson, C., and Kouzarides, T. (2004). Histone H3 lysine 4 methylation patterns in higher eukaryotic genes. Nat. Cell Biol. *6*, 73–77.

Sims, R.J., 3rd, Nishioka, K., and Reinberg, D. (2003). Histone lysine methylation: a signature for chromatin function. Trends Genet. *19*, 629–639.

Smith, E.R., Pannuti, A., Gu, W.G., Steurnagel, A., Cook, R.G., Allis, C.D., and Lucchesi, J.C. (2000). The *Drosophila* MSL complex acetylates histone h4 at lysine *16*, a chromatin modification linked to dosage compensation. Mol. Cell. Biol. *20*, 312–318.

Smith, E.R., Allis, C.D., and Lucchesi, J.C. (2001). Linking global histone acetylation to the transcription enhancement of X-chromosomal genes in Drosophila males. J. Biol. Chem. *276*, 31483–31486.

Smith, C.M., Gafken, P.R., Zhang, Z., Gottschling, D.E., Smith, J.B., and Smith, D.L. (2003). Mass spectrometric quantification of acetylation at specific lysines within the amino-terminal tail of histone H4. Anal. Biochem. *316*, 23–33.

Strahl, B.D., and Allis, C.D. (2000). The language of covalent histone modifications. Nature *403*, 41–45.

Strahl, B.D., Ohba, R., Cook, R.G., and Allis, C.D. (1999). Methylation of histone H3 at lysine 4 is highly conserved and correlates with transcriptionally active nuclei in tetrahymena. Proc. Natl. Acad. Sci. USA *96*, 14967–14972.

Turner, B.M. (2002). Cellular memory and the histone code. Cell *111*, 285–291.

Turner, B.M., Birley, A.J., and Lavender, J. (1992). Histone H4 isoforms acetylated at specific lysine residues define individual chromosomes and chromatin domains in Drosophila polytene nuclei. Cell *69*, 375–384.

Vaquero, A., Loyola, A., and Reinberg, D. (2003). The constantly changing face of chromatin. Sci. Aging Knowledge Environ. *2003*, RE4.

Wysocka, J., Myers, M.P., Laherty, C.D., Eisenman, R.N., and Herr, W. (2003). Human Sin3 deacetylase and trithorax-related Set1/Ash2 histone H3-K4 methyltransferase are tethered together selectively by the cell-proliferation factor HCF-1. Genes Dev. *17*, 896–911.

Wysocka, J., Swigut, T., Milne, T.A., Dou, Y., Zhang, X., Burlingame, A.L., Roeder, R.G., Brivanlou, A.H., and Allis, C.D. (2005). WDR5 associates with histone H3 methylated at K4 and is essential for H3 K4 methylation and vertebrate development. Cell *121*, this issue, 859–872.

Yokoyama, A., Wang, Z., Wysocka, J., Sanyal, M., Aufiero, D.J., Kitabayashi, I., Herr, W., and Cleary, M.L. (2004). Leukemia proto-oncoprotein MLL forms a SET1-like histone methyltransferase complex with menin to regulate Hox gene expression. Mol. Cell. Biol. *24*, 5639–5649.

Yu, B.D., Hess, J.L., Horning, S.E., Brown, G.A., and Korsmeyer, S.J. (1995). Altered Hox expression and segmental identity in Mll-mutant mice. Nature *378*, 505–508.

Zhang, K., Siino, J.S., Jones, P.R., Yau, P.M., and Bradbury, E.M. (2004). A mass spectrometric "Western blot" to evaluate the correlations between histone methylation and histone acetylation. Proteomics *4*, 3765–3775.

Zhang, K., Williams, K.E., Huang, L., Yau, P., Siino, J.S., Bradbury, E.M., Jones, P.R., Minch, M.J., and Burlingame, A.L. (2002). Histone acetylation and deacetylation: identification of acetylation and methylation sites of HeLa histone H4 by mass spectrometry. Mol. Cell. Proteomics *1*, 500–508.